ELSEVIER

Experimental study of turbulent flow in the near wakes of single and tandem prisms

R. Devarakonda and J. A. C. Humphrey
Department of Aerospace and Mechanical Engineering, University of Arizona, Tucson, AZ, USA

An experimental study was performed for the flow of air normal to a prism of square cross section (side dimension D and length H) spanning a duct of square cross section (side dimension H). Two prism arrangements were investigated corresponding to: (1) the prism of side D on its own, at different distances α ($=a/H$) from the bottom duct wall; and, (2) the prism of side D with a second, smaller prism of side δ ($=d/D$) placed upstream, parallel to and in line with it. In both arrangements, the top and bottom surfaces of the prisms were aligned parallel to the top and bottom walls of the duct. In the second arrangement, the longitudinal axes of the prisms were always contained in the horizontal symmetry plane of the duct ($\alpha = 0.50$) and the center-to-center interprism distance λ ($=L/D$) was varied. Laser-Doppler velocimetry (LDV) was used to measure the mean and rms streamwise velocity components at various streamwise locations along traverses contained in the vertical symmetry plane of the duct normal to the axes of the prisms. These data were obtained for a value of the Reynolds number $Re_D = 1.0 \times 10^4$ ($Re_D = U_i D/v$, where U_i is the average velocity of the air at the duct inlet, and v its kinematic viscosity). Lift and drag coefficients, as well as the Strouhal number ($St_D = fD/U_i$, where f is the vortex-shedding frequency in Hz), were also determined for the prism of side D for values of the Reynolds number equal to 1.0×10^4, 2.0×10^4 and 2.75×10^4. The measurements of the above quantities reveal a significant dependence of the flow on all the parameters investigated, with large differences arising between the single and tandem prism arrangements. For the tandem arrangements with $\delta < 1.0$, the downstream prism experiences a decrease in drag and an increase in vortex-shedding frequency (relative to the single-prism case) that varies with λ. For the single-prism arrangement, decreasing the wall distance α to values $\alpha < 0.20$ significantly decreases the drag coefficient while increasing the lift coefficient and the Strouhal number. In addition to their intrinsic value, the measurements provide modest but challenging targets for testing numerical calculations of single and interacting near-wake turbulent flows.

Keywords: bluff bodies; obstructions; wake flows; turbulence

Introduction to the problem

Turbulent slows past two-dimensional (2-D) bluff bodies of various cross sections have been the subject of considerable research for may years. See, among others, Žukauskas (1972); Zdravkovich (1977); Ota et al. (1986); Igarashi (1985, 1986, 1987). Of special interest are the structure and dynamics of bluff body wakes as a function of Reynolds number. This class of flows is also of considerable practical importance, because many engineering components and structures (such as heat exchangers, off-shore oil rigs, transmission lines, moving vehicles, smoke stacks, and buildings) require, for design purposes, an understanding of the characteristics of these flows, especially in relation to the forces the flows induce upon the objects affected.

Address reprint requests to Prof. J. A. C. Humphrey, Dept. of Aerospace and Mechanical Engineering, University of Arizona, Aero Building 16, Tucson, AZ 85721, USA.

Received 9 December 1995; accepted 29 February 1996

Int. J. Heat and Fluid Flow 17: 219–227, 1996

655 Avenue of the Americas, New York, NY 10010

0142-727X/96/$15.00
PII S0142-727X(96)0029-5

The literature on single and interacting bluff body turbulent flows has been reviewed by Devarakonda (1994) to whom the reader is referred. The main issues of interest are summarized here. Of the different cross sections, circular cylinders and rectangular/square prisms have received the most attention. Cylinders in different types of flow configurations (single cylinders; cylinder pairs in tandem or offset arrangements; cylinder banks in staggered and in-line arrays) have been studied, with emphasis placed on resolving the effects of Reynolds number and relative orientation on flow-field structure, cylinder surface pressure distribution, drag, lift, Strouhal and Nusselt numbers. Other single-cylinder investigations have addressed the influence of the proximity of a wall on heat transfer, drag, lift, and vortex shedding as well as the effects of free-stream turbulence on these quantities.

In contrast to single prisms, there is comparatively little information on the flow past prisms of rectangular/square cross section in tandem arrangements. Notable exceptions are the investigations by Tatsutani et al. (1993), Luo and Teng (1990), and Sayers (1991). However, the sparseness of information as well as the discrepancies and knowledge gaps among investiga-

tions such as these point to a lack of understanding of this flow configuration. Certainly, the information available for pairs of circular cylinders in tandem arrangements (Zdravkovich 1977) can be looked to for guidance, but special care must be taken to identify those features of bluff body flows which are strongly dependent on geometry, such as the separation points which are fixed on prisms but can meander on cylinders.

In this communication, we examine various time-averaged features associated with the near-wake flow downstream of a single prism or downstream of a pair of prisms in tandem. Mean and rms velocities, individual surface forces, and flow oscillation frequencies are determined for different prism size ratios and interprism separations primarily for one value of the Reynolds number. With reference to Figure 1, which shows the most general case, an experiment has been performed for the isothermal flow of air past a pair of prisms located a distance L apart in the horizontal symmetry plane of a duct of square cross section (dimension $H = 16$ cm). Both prisms are of length H normal to the plane of the figure. The larger one has side dimension $D = 2.20$ cm and is always downstream of the smaller one of side dimension d. The longitudinal axes of the prisms are aligned parallel to each other and normal to the bulk flow. The top and bottom surfaces of each prism are always parallel to the top and bottom walls of the duct.

We have investigated flows corresponding primarily to $\delta = 0.25$, 0.50, and 1.0 for interprism spacings of $\lambda = 1.0$, 2.0, 3.0, and 4.0 with $\alpha = 0.50$. Also of interest has been the flow past a single prism of side D for prism-wall distances corresponding to $\alpha = 0.07$, 0.20, 0.35, and 0.50. The Reynolds number Re_D, the Strouhal number St_D, and the geometrical parameters α, δ, and λ are as defined in the Abstract.

Transverse profiles of the mean and rms values of the streamwise component of velocity, obtained at various streamwise locations in the vertical symmetry plane normal to the prisms, have been derived from corresponding time records of velocity measured with a laser Doppler velocimeter (LDV). Also measured for both the single and tandem cases are the Strouhal number, the drag C_D ($= F_D/0.5\rho U_i^2 D$), and the lift C_L ($= F_L/0.5\rho U_i^2 D$) coefficients for the larger prism. In the latter expressions, F_D and F_L are the time-averaged net pressure forces per unit length acting in the streamwise and transverse directions, respectively.

The bulk of the data, including all the velocity and Strouhal number measurements, has been obtained for $Re_D = 1.0 \times 10^4$. Values for the drag and lift coefficients corresonding to the single larger prism have also been obtained for $Re_D = 2.0 \times 10^4$ and 2.75×10^4. As discussed below, checks showed that the flow in the duct at the measurement locations was essentially two-dimensional (2-D).

The experiment

Apparatus

The experiments were performed in the test section of a low-speed (subsonic) open-loop wind tunnel designed and constructed especially for this investigation. A detailed description of the apparatus and its associated instrumentation is provided in Devarakonda (1994). The wind tunnel consists of four sections: the blower, the flow-conditioning section, the test section, and the outlet section. The air flow is provided by a backward-inclined squirrel cage blower driven by a 5-HP, 208-V, 3-phase motor. The flow-conditioning section was designed to minimize temporal and spatial fluctuations in the flow. It is composed of a wide-angle diffuser, a settling chamber containing honeycomb, a settling chamber containing aluminum screens, and a flow-contracting nozzle with an inlet-to-outlet area ratio of 9:1. The dimensions of the various flow conditioning parts were determined following the recommendations of Mehta and Bradshaw

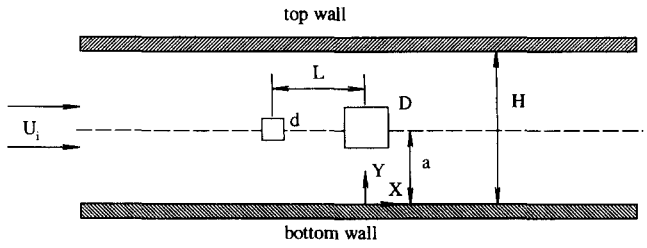

Figure 1 Flow configuration showing small (d) and large (D) prisms in the horizontal symmetry plane of a duct of square cross section (H); for the case of a single prism (D), the distance a is variable; for the case of prism pairs in tandem, d and L are variables, $\alpha = a/H = 0.50$ is fixed, and the small prism is always located upstream of the large one

(1979). The nozzle profile was calculated according to the inviscid flow design procedures of Cohen and Ritchie (1962) and Albayrak (1991). The nozzle contraction is followed by the test section, and this by a gently linearly expanding diffuser through which air is dumped into the surroundings with minimum disturbance to the flow in the test section.

The test section is a duct, 73.5 cm long and 16 cm × 16 cm of inner square cross section, constructed from four acrylic sheets of 1.27 cm thickness joined by regularly spaced screws and sealed with teflon tape. The prisms placed in the test section were made of stainless steel in the case of the upstream prisms and of acrylic in the case of the larger downstream prism. The downstream prism has eight evenly spaced pressure taps drilled in-line along the width of one of its four surfaces, half-way along its length. This prism was fixed to a slider and could be placed at any value of Y/D with its axis contained in the Y–Z plane located at $X/D = 10.91$ downstream of the test section inlet. The small prisms were always located at $Y/H = 0.5$ and were fixed in place by a very slight compression of the duct side walls.

Velocity, pressure, and frequency measurements

Measurements of the streamwise velocity component were made using the green channel of a two-component DANTEC 55X LDV arranged in forward-scatter mode. A coherent Innova model 990-5 Argon-ion 2-W laser provided the 488-nm light source. The use of a 310-mm front lens with a beam half-angle of 4.3° yielded a $1/e^2$ probe volume of dimensions $1 \times 0.1 \times 0.1$ mm^3, approximately. The probe volume contained about 30 fringes spaced 3 μm apart. The optical unit was attached to a computer controlled traversing mechanism that allowed the probe volume to be displaced up to a distance of 600 mm in each of three mutually orthogonal directions with a precision of $\pm 1/240$ mm. The electronics associated with the LDV system include a DANTEC 55L90 counter processor, a DANTEC 55N14 electronic frequency shifter (used in conjunction with a Bragg cell), and a DANTEC 55G20 buffer interface connected to an IBM PC-AT through a GPIB interface board.

Water droplets of diameter less than 5 μm were used as the flow-seeding agent. The droplets were generated using a Sonic Environmental Systems air-blast atomizer. The atomizer was located in the upstream section of the wide-angle diffuser preceding the settling chambers. Careful checks of the flow in the test section revealed no measurable distortions of the mean or rms velocities that could be attributed to the atomizer. Validated Doppler burst datarates in excess of 800 Hz were obtained with this arrangement.

Drag and lift coefficients were determined from pressure measurements made on the larger, downstream prism. Teflon tubes of outer diameter 0.965 mm and inner diameter 0.580 mm were strung along the hollow center of the prism to connect the

eight in-line pressure taps on one surface of the prism to a carefully calibrated Validyne variable reluctance pressure transducer. The pressure measurements were made one pressure tap at a time. The peripheral variation of pressure was determined by rotating the prism in 90° increments with respect to the approaching flow. The drag coefficient was determined by taking the difference between the time-averaged values of pressure acting on the front and back prism surfaces. (The total force acting on one side of a prism F_S was determined by summing the products of time-averaged pressure times area for each tap.) The lift coefficient was determined similarly, from the time-averaged values of pressure acting on the top and bottom surfaces of the prism. In the experiment, it was only possible to determine the pressure contribution to C_D and C_L, but for $Re_D \geq 1.0 \times 10^4$ the shear contribution to these quantities is expected to be small.

For most of the pressure measurements, the instrumentation reached steady state almost instantaneously and did not show fluctuations larger than $\pm 1\%$ about the mean. Typical vortex-shedding frequencies determined from the velocity records varied from 30 to 70 Hz. Although the pressure transducer was capable of detecting fluctuations of up to 500 Hz, the signals received were not sufficiently resolved to determine these vortex-shedding frequencies. It must be concluded that the amplitude response of the entire pressure-sensing system was not sensitive enough to measure pressure fluctuations corresponding to vortex shedding. Notwithstanding, the magnitudes of the fluctuations about the mean were noted and incorporated in the uncertainty analysis. The Strouhal number was determined from spectra of the velocity records obtained $5D$ downstream of the large prism.

Measurement procedure and uncertainties

The downstream prism was held in a mechanical mount and could be positioned in the Y-coordinate direction to within ± 2 mm. Similarly, with care, the small prisms could also be aligned to within ± 2 mm along the X and Y coordinate directions. The data processed by the LDV system software were time records of the streamwise velocity component for various probe locations. Processing included statistical and spectral analyses of the time records from which mean and rms velocities as well as autocorrelations and power spectra were obtained. Because the mean and rms velocities were obtained from discretized forms of the time-average definitions, velocity bias was essentially removed from these quantities; see Drain (1980). The slotted autocorrelation technique attributable to Bell (1986) was used to obtain the energy spectra.

The uncertainty analysis follows Kline and McClintock (1953) and Moffat (1982). Measurements relating to lengths were known to within $\pm 5\%$. Errors in probe volume location and beam angle were mainly due to uncertainties in the alignment of the LDV system relative to the walls of the test section. The traverse system was aligned parallel to the walls of the test section to within $\pm 1.5\%$. Each mean and rms value of velocity was based on at least 3950 validated Doppler bursts out of a maximum of 4000 bursts. In addition, to quantify measurement reproducibility in this highly unsteady flow, at each measurement location data were collected two to three times. Single values of the mean and rms velocities were determined to within $\pm 5\%$. The other sources of uncertainty combined affecting velocity amounted to less than the repeatability uncertainty, which varied from ± 1 to $\pm 5\%$ (see Devarakonda 1994).

The pressure measurements were made with respect to atmospheric pressure with the water atomizer turned off. (This resulted in a 5°C temperature increase relative to the air with droplets. Thus, because of the effect on viscosity, for the same inlet velocity the Reynolds number of the atomized flow was about 7.6% higher than that for the unatomized flow. The values of Reynolds quoted here refer to atomized flows.) The calibrated pressure transducer is accurate to ± 1.2 Pa. The pressure measurements varied from 10 to 470 Pa for the parameter range explored. For pressure measurements of the order of 10 Pa, the accuracy of the pressure transducer was the dominant source of uncertainty. For the measurements made in the 200–470 Pa range, the chief contribution to uncertainty was flow unsteadiness. The overall uncertainty in the pressure measurements ranged form ± 1 to $\pm 12\%$. The associated uncertainties in C_D and C_L were found to vary from ± 3.1 to $\pm 12.7\%$.

The errors affecting the values of vortex-shedding frequency were attributable to the finite lengths of the velocity records and the uncertainty associated with determining values of frequency

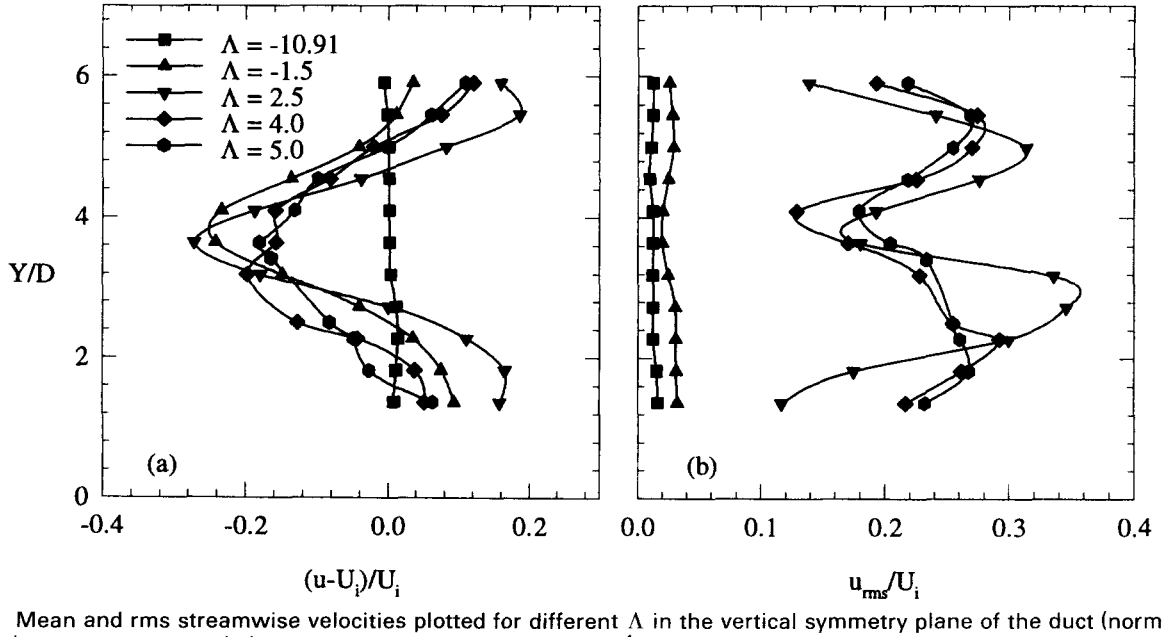

Figure 2 Mean and rms streamwise velocities plotted for different Λ in the vertical symmetry plane of the duct (normal to the prism axis) for a single prism (D) with $\alpha = 0.50$ and $Re_D = 1.0 \times 10^4$

from the corresponding power spectra. The dominant frequency was measured several times for each prism configuration, and the spread in these values was used to estimate the uncertainty. For the parameter range investigated, the uncertainty in frequency was found to vary from ± 1 to $\pm 3\%$. The associated uncertainty in St_D varied from ± 2.7 to $\pm 6.3\%$.

The effect on the mean flow attributable to boundary-layer growth along the duct walls and the blockage of the prisms was estimated for the single large prism. The boundary-layer thickness on one wall of the duct was calculated to be $Y/H|_D = 0.057$ for $Re_D = 1 \times 10^4$ at the large prism location. Combined with the blockage attributable to the large prism ($D/H = 0.138$), this is estimated to have increased to about $1.5U_i$ the value of the average velocity of the flow past the large prism. Notwithstanding, because the velocity increase could not be determined exactly, we have employed U_i as the reference velocity for nondimensionalization purposes.

Results and discussion

All results are presented in nondimensional form. The time-averaged streamwise velocity component u is scaled according to $(u - U_i)/U_i$, the rms velocity is scaled with U_i, distances along Y are scaled with D, and distances along X are scaled with d or D, as appropriate. The time-averaged drag and lift coefficients defined above C_D and C_L were determined only for the downstream prism (D), whether in single or tandem arrangements.

The velocity measurements for the different configurations included collecting data: (1) along vertical traverses contained in the vertical symmetry plane of the duct, perpendicular to the axes of the prisms and half-way along their length; and, (2) along the horizontal centerline of the duct, upstream and downstream of the single or tandem prism arrangements. All velocity measurements correspond to the streamwise velocity component, and a cubic spline was used to fit curves through the datapoints in the figures.

The main results obtained for a single prism placed at different distances α from the bottom wall of the duct are discussed first. Those for a pair of prisms in tandem follow. For the latter case, three prism diameter ratios ($\delta = 0.25$, 0.50, and 1.00) and two interprism spacings (λ) were considered. For $\delta = 1.0$, the two values of λ were 1.5 and 4.0, and for $\delta = 0.25$ and 0.50, the values of λ were set to 1.0 and 4.0. Intermediate values of λ corresponding to 2.0 and 3.0 were also set in the experiments for determining C_D and St_D. Except for where explicitly stated, all measurements were taken at $Re_D = 1 \times 10^4$.

Single prism in cross flow

Mean and rms velocity profiles measured at five streamwise locations Λ ($= X/D$) in the vertical symmetry plane of the duct are plotted in Figure 2a and b for the case with $\alpha = 0.50$. In the plot, the coordinates ($X/D = 0.00$, $Y/D = 3.64$) denote the geometrical center of the prism, which, in this case, is contained in the horizontal symmetry plane of the duct. The results show that both the mean and rms velocities are uniform to within $\pm 1.6\%$ at the test section inlet plane ($\Lambda = -10.91$), the latter quantity nowhere exceeding 0.017. Checks on the mean and rms velocities at $\Lambda = 2.5$ also showed these to be uniform, to within $\pm 3.0\%$, in the spanwise direction (along the length of the prism) in regions $\pm 2D$ above and below the horizontal symmetry plane.

At $\Lambda = -1.5$, the mean and, to a much smaller extent, the rms already show the influence of the prism on the approaching flow. By $\Lambda = 2.5$, the rms has increased markedly, maximizing in the shear layers originating along the top and bottom surfaces of the prism. Downstream of the prism, the outer edges of the shear layers have spread out significantly in the transverse direction. Relative to a virtual origin located at about $\Lambda = -0.8$, the half-angle at which the wake spreads, as characterized by the transverse displacement of the peaks in the rms profiles, is $\beta = 18.5° \pm 1.0°$. Table 1a shows that the vortex-shedding frequency measured for this case was $St_D = 0.136$, and it is reasonable to assume that energetic, large-scale (nonturbulent) flow oscillations contribute to the high values of the rms in the shear layers. Although the magnitude of this contribution to the total rms has not been determined in our work, it is an item of increasing interest in numerical simulations of this class of flows. See, for example, Franke and Rodi (1991) and Bosch and Rodi (1995).

Plots of the mean and rms velocities measured at $\Lambda = 2.5$ and 5.0 for configurations with $\alpha = 0.35$ and 0.20, respectively, are available in Devarakonda (1994) for readers requiring quantitative values. Because the qualitative outcomes are as expected, we simply summarize them here. Placing the prism closer to the duct wall induces an asymmetry in the flow relative to the horizontal symmetry plane. The asymmetry is evidenced by increasingly altered shapes and magnitudes of the mean and rms profiles with increased proximity of the prism to the duct wall. Relative to the symmetrical flow configuration with $\alpha = 0.50$, the asymmetric profiles display lower values of the mean velocity in the wake of the prism and higher relative values of the rms in the reduced prism–duct wall space.

Energy spectra were derived from the velocity records measured at $\Lambda = 5$ at transverse locations $1D$ from the top or bottom surfaces of the prism. The Strouhal numbers calculated from the values of frequency obtained from the spectra are given in Table 1a. These data show that between $\alpha = 0.50$ and 0.20, the value of St_D increases from 0.136 to 0.154. The value of $St_D = 0.136$ for the prism located on the horizontal symmetry plane ($\alpha = 0.50$) is in good agreement with the measurements of Okajima (1982) and Durão et al. (1988) who both find $St_D = 0.13$. Although not determined here for lack of sufficiently high data rates, nearer to the duct wall ($\alpha < 0.20$), the value of St_D is expected to diminish to values smaller than the centerline value. For example, Bosch and Rodi (1995) report nonvortex-shedding flow at $Re_D = 2.2 \times 10^4$ in the wake of a prism with $\alpha < 0.1$ in a channel.

The force (F_S) acting on each surface of the prism was derived from the measurements of pressure for each surface. Figure 3 shows the results plotted as a function of α for the case with $Re_D = 1.0 \times 10^4$. (The negative values in the figure simply reflect the arbitrary choice of the reference pressure. Mentally adding a constant to these results, so that they are all positive, facilitates their qualitative interpretation.) For the symmetrical configuration with $\alpha = 0.50$, the force is largest on the front surface of the prism, that facing the approaching flow, and much lower on the rear or back surface as the result of the incomplete pressure recovery in the wake. The forces acting on the top and bottom surfaces are equal, and smaller than the force acting on the rear surface because of the higher speed of the flow past these surfaces (relative to the wake), which lowers the pressure acting on them (relative to the back surface).

The data show that displacing the prism from the horizontal symmetry plane ($\alpha = 0.50$) to a location fairly close to the wall ($\alpha = 0.07$) works to monotonically increase, although only moderately, the magnitudes of the forces acting on the back and top surfaces of the prism, respectively. In contrast, the forces acting on the front and bottom surfaces vary nonmonotonically, with the magnitude of the force on the bottom surface increasing markedly in moving from $\alpha = 0.20$ to 0.07.

These results help clarify the interesting variations in the drag and lift coefficients plotted as a function of α in Figure 4a and 4b. (Note that in the definitions used to calculate C_D and C_L, the drag and lift forces are $F_D = F_{FRONT} - F_{REAR}$ and $F_L =$

Table 1 Strouhal numbers at $Re_D = 1.0 \times 10^4$ for: (a) single prism of square cross section placed at different α; (b) two prisms placed in tandem in the duct horizontal symmetry plane*

(a)

α	St_D
0.50	0.136
0.35	0.144
0.20	0.154
0.07	—

(b)

	St_D		
λ	$\delta = 0.25$	$\delta = 0.50$	$\delta = 1.00$
1.0 (1.5)	0.158	0.245	0.131
2.0 (2.5)	—	0.210	0.111
3.0	—	—	0.112
4.0	—	—	0.131

*Values of α in parentheses correspond to $\delta = 1.00$; interrupted lines (---) indicate that a flow oscillation frequency could not be unambiguously determined. The uncertainty in St_D varies from $\pm 2.7\%$ to $\pm 6.3\%$

$F_{BOTTOM} - F_{TOP}$, respectively.) In moving the prism from $\alpha = 0.20$ to 0.07, toward the duct wall, C_D decreases, and C_L increases significantly for the three values of Re_D explored. In the case of C_D, this is due to an increase in pressure on the back surface relative to that on the front surface, resulting in a reduced net force acting in the positive X-direction. In the case of C_L, the large pressure increase on the bottom surface of the prism relative to the top results in an increased net force acting in the positive Y-direction. As expected, to within the measurement uncertainty, the value of C_L becomes zero at $\alpha = 0.50$. Present measurements with $\alpha = 0.50$ yield $C_D = 2.1$ for $Re_D = 1.0 \times 10^4$ and 2.28 for $Re_D = 2.0 \times 10^4$ and 2.75×10^4, respectively. These values agree well with those obtained by Igarashi (1986) and Lee (1975), 2.25 and 2.18, respectively, and sustain the observation made by Bearman and Obasaju (1982) that C_D does not change appreciably for $Re_D > 2.0 \times 10^4$.

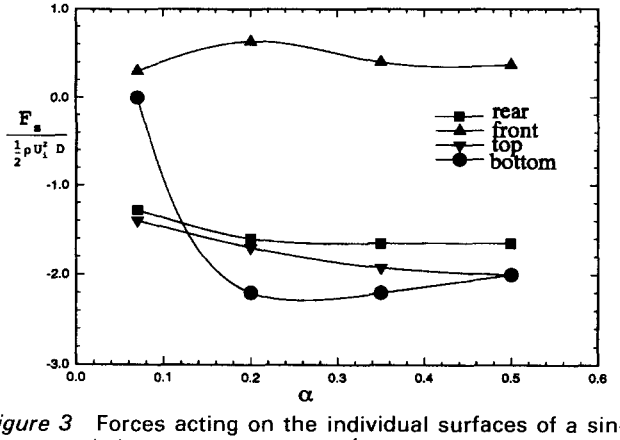

Figure 3 Forces acting on the individual surfaces of a single prism (D) with $Re_D = 1.0 \times 10^4$, plotted as a function of α; the forces were determined from pressure measurements and negative values reflect the (arbitrary) origin of fixed reference pressure

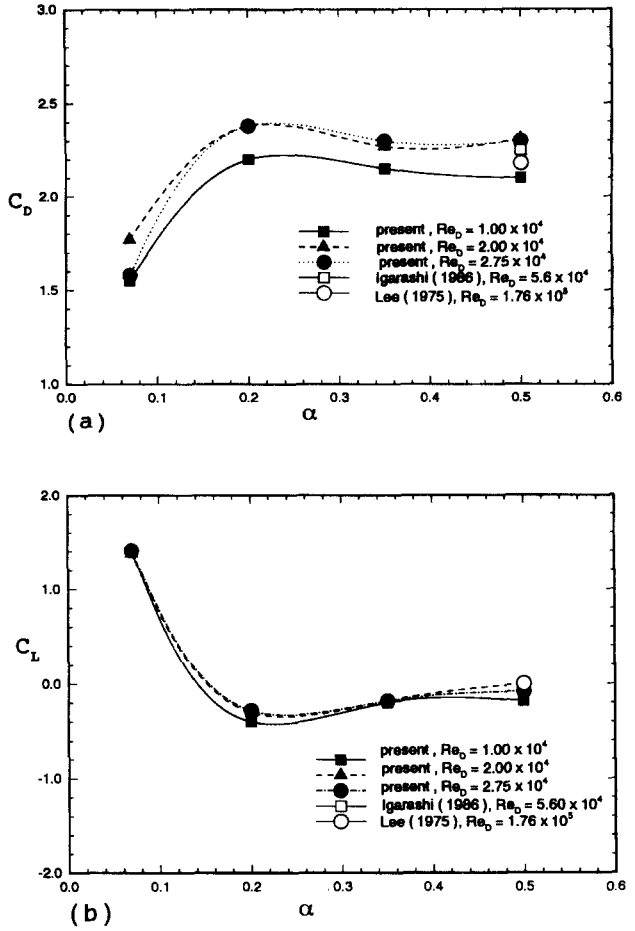

Figure 4 Drag (a) and lift (b) coefficients for a single prism (D) plotted as a function of α for three values of Re_D

Around $\alpha = 0.20$, both C_D and C_L display noteworthy features. C_D maximizes near $\alpha = 0.20$ and then decreases asymptotically to its limiting (centerline) value at $\alpha = 0.50$. In contrast, C_L minimizes and becomes *negative* near $\alpha = 0.20$ and then increases asymptotically to its limiting (centerline) value of zero at $\alpha = 0.50$. The negative value of C_L denotes a reversal in the sense of the lift force acting on the prism, which, for $0.20 < \alpha < 0.50$, appears to be directed *toward* the duct wall as opposed to away from it.

These interesting variations in the drag and lift coefficients coincide with a marked variation in the Strouhal number in the same range of α (see Table 1a). Although the data we have obtained are insufficient to provide a definitive theoretical interpretation of these findings, it seems reasonable to suggest that an explanation connecting them is likely to be found in the transition from a slightly asymmetric wake structure (with weak duct wall interactions) when $0.20 < \alpha < 0.50$ to a strongly asymmetric structure (with strong duct wall interactions) when $\alpha < 0.20$.

Tandem prisms in cross flow

Mean and rms velocity profiles for the tandem-prism arrangements are shown in Figure 5. Compared to a single prism (Figure 2a), the reduction in centerline velocity at $\Lambda = 2.5$ and 5.0 is always larger for tandem-prism pairs, the effect being most pronounced for the largest interprism separation $\lambda = 4.0$. With decreasing prism size ratio δ, the velocity deficit region (where $(u - U_i)/U_i < 0$) significantly decreases in its transverse dimen-

sion, and both the mean and rms distributions are more precisely (symmetrically) defined. These effects are already noticeable when δ is reduced from 1.00 to 0.50.

Figure 6 shows the mean and rms velocities measured along the centerline of the duct, upstream and downstream of a single prism ($\delta = 0$), and similarly for a pair of prisms in tandem with interprism separation $\lambda = 4.0$. (Note the X/d and X/D scalings used upstream and downstream of the prism(s), respectively.) In the upstream region, the mean and rms profiles for the prisms in tandem are very similar to the single-prism case. Defining the "extent of influence" as the upstream location where the nondimensional profiles change by 5% of their free-stream values, then the influence of a prism pair is felt between $X/d = -5$ and -3 for the mean velocity and between $X/d = -3$ and -2 for the rms. Especially noteworthy are the relatively large increases in the rms of the flow approaching the front surface of the upstream prism (between $X/d = -2$ and 0). Given the low level of turbulence intensity in the approaching flow, this localized increase in the fluctuating component of motion is attributed to the unsteadiness of the flow in the vicinity of the stagnation point on the front surface of the upstream prism, which is influenced by vortex shedding from the prisms.

For $X/D > 1.0$, the mean velocity profiles for the prism pairs in tandem are fairly similar but differ significantly from the single-prism case, the values of velocity for the tandem arrangements always being smaller than for a single prism. Thus, flow recovery in the wake of a prism pair is considerably slower than for a single prism. These data also show that both the intensity and extent of the reversed flow along the centerline in the wake of a prism pair increase with decreasing δ. For $X/D < 2.0$, the rms values for the tandem arrangements are smaller than those for the single prism; whereas, for $2.0 < X/D < 6.0$, the reverse is true. For $X/D > 6.0$, the rms values for the single- and tandem-prism arrangements converge to essentially the same value ($u_{rms}/U_i \approx 20\%$), which is approximately 17 times larger than the rms of the approaching flow.

The drag coefficient for the downstream prism in tandem arrangements with $\mathrm{Re}_D = 1.0 \times 10^4$ was determined from surface pressure measurements, as explained above. Figure 7 shows C_D as a function of interprism spacing λ for different prism size ratios δ. (Also included is the datum $C_D = 2.1$ for the single-prism case ($\delta = 0$), the largest value measured.) For $\lambda < 2$, approximately, the drag coefficient decreases markedly with increasing δ, to the point where, for $\delta = 0.50$ and, especially, $\delta = 1.0$, the net drag force on the downstream prism is directed counter to the bulk flow direction ($C_D < 0$). A similar finding is reported for tandem cylinders by Zdravkovich (1977), who attributes the drag reduction to an improved streamlining of the flow past the cylinder pair. However, for larger values of λ, the value of C_D for the tandem prisms with $\delta = 1.0$ quickly rises to the single-prism value while the values for $\delta = 0.25$ and 0.50 level out to $C_D \approx 0.8$. It is clear from the plots that for interprism spacings $\lambda > 2$, decreasing the size of the upstream prism works to significantly reduce the drag on the larger downstream prism, while the converse is true for $\lambda < 2$. In all of these cases, $\alpha = 0.50$ and the lift coefficient C_L of the downstream prism was zero to within experimental uncertainty.

The Strouhal number was also determined for the downstream prism of a pair in tandem with $\mathrm{Re}_D = 1.0 \times 10^4$. Because U_i and D were the same for all the cases examined, differences in St_D are entirely due to the upstream/downstream prism interactions. The results are given in Table 1b, and we tentatively conclude that for $\lambda \approx 1$, the Strouhal number maximizes between $\delta = 0.25$ and 1.00; whereas, for $\delta \approx 1.00$, it minimizes between $\lambda = 1.0$ and 4.0. In particular, the value of $\mathrm{St}_D = 0.245$ corresponding to $\delta = 0.50$ when $\lambda = 1.0$ was the largest observed. This is nearly twice the value for the single prism (0.136), and it is reasonable to ask: Does the upstream prism (d) drive the vortex shedding frequency of the downstream prism (D)? To provide a rigorous answer to this question, St_d and St_D should be known as a function of λ for this δ and Re_D, and we have but two measurements of St_D at $\lambda = 1.0$ and 2.0, respectively. Notwithstanding, we note that *if* prism d drives prism D in a tandem pair, then we should expect $f_d = f_D$ for some λ, with the consequence (from the definition of the Strouhal number) that $\mathrm{St}_D/\mathrm{St}_d = \{U_i|_d/U_i|_D\}\{D/d\}$. Because $U_i|_d = U_i|_D$ (the inlet velocity used in the definition of Strouhal is independent of the prism cross section dimension) it follows that $\mathrm{St}_D/\mathrm{St}_d = 1/\delta = 2.0$ for some λ at $\delta = 0.50$. To test this result, we take for St_d the measured value 0.136 for the single prism located on the horizontal symmetry plane (Table 1a), and for St_D the measured value 0.245 (Table 1b) to find $\mathrm{St}_D/\mathrm{St}_d = 1.8$ at $\lambda = 1.0$. This result is close to the expected value of 2.0. For $\delta = 1.0$, we expect $\mathrm{St}_D/\mathrm{St}_d = 1.0$ and find 0.96 when $\lambda = 1.5$ and 4.0. For $\delta = 0.25$, we expect $\mathrm{St}_D/\mathrm{St}_d = 4.0$ but have insufficient results to check this case.

Although sparse, the Strouhal number results support the following two notions: (1) the vortex-shedding frequency of the downstream prism of a tandem pair with $\delta \leq 1.0$ differs significantly from that for a single prism due to upstream/downstream prism interactions; and (2) the upstream prism of the same tandem pair can drive the vortex-shedding frequency of the downstream prism for certain values of λ. Additional support for both of these statements can be found in the review by Zdravkovich (1977) on flow interference effects between tandem cylinders of equal circular cross section. In particular, and as in the present study, the author reports that between $\lambda = 2.0$ and 3.8, approximately, the Strouhal number of the downstream cylinder of a pair is smaller than for a single cylinder, and that for $\lambda > 3.8$ the Strouhal number of the downstream cylinder quickly approaches the single cylinder value with the two cylinders shedding vortices synchronously.

Conclusions

Present findings reveal the extent to which the flow of air around a prism of square cross section, aligned normal to the streamwise component of motion through a duct, is altered as a function of prism–wall distance, or as a function of a second prism placed upstream and parallel to it when both prisms are contained in the duct symmetry plane. Streamwise velocity component time records measured with an LDV yield Strouhal numbers as well as mean and rms values of velocity at various locations in the flow. The mean and rms velocity measurements show that placing a small prism upstream and in line with a larger prism significantly streamlines the flow. Drag and lift coefficients have also been determined from pressure measurements obtained around the larger downstream prism. Combined, the velocity, drag, lift, and frequency data provide a modest but challenging target for numerical simulations of this class of flows.

The pressure measurements for a single prism with $\alpha \leq 0.2$, approximately, show that drag decreases and lift increases with decreasing α. Between $\alpha = 0.2$ and 0.3, drag maximizes and lift minimizes, the latter quantity becoming slightly less than zero to indicate that the lift force is then directed towards the duct wall as opposed to away from it. The Strouhal number for a single prism is observed to increase with decreasing α in the range $0.20 < \alpha < 0.50$.

Relative to a single prism, the drag on the downstream prism of a pair in tandem can be significantly reduced. This variation in drag with prism size ratio δ and interprism separation λ is nonmonotonic. For $\lambda < 2$, approximately, the drag coefficient decreases markedly with increasing δ, to the point where, for $\delta = 0.50$ and $\delta = 1.0$ the net drag force on the downstream prism

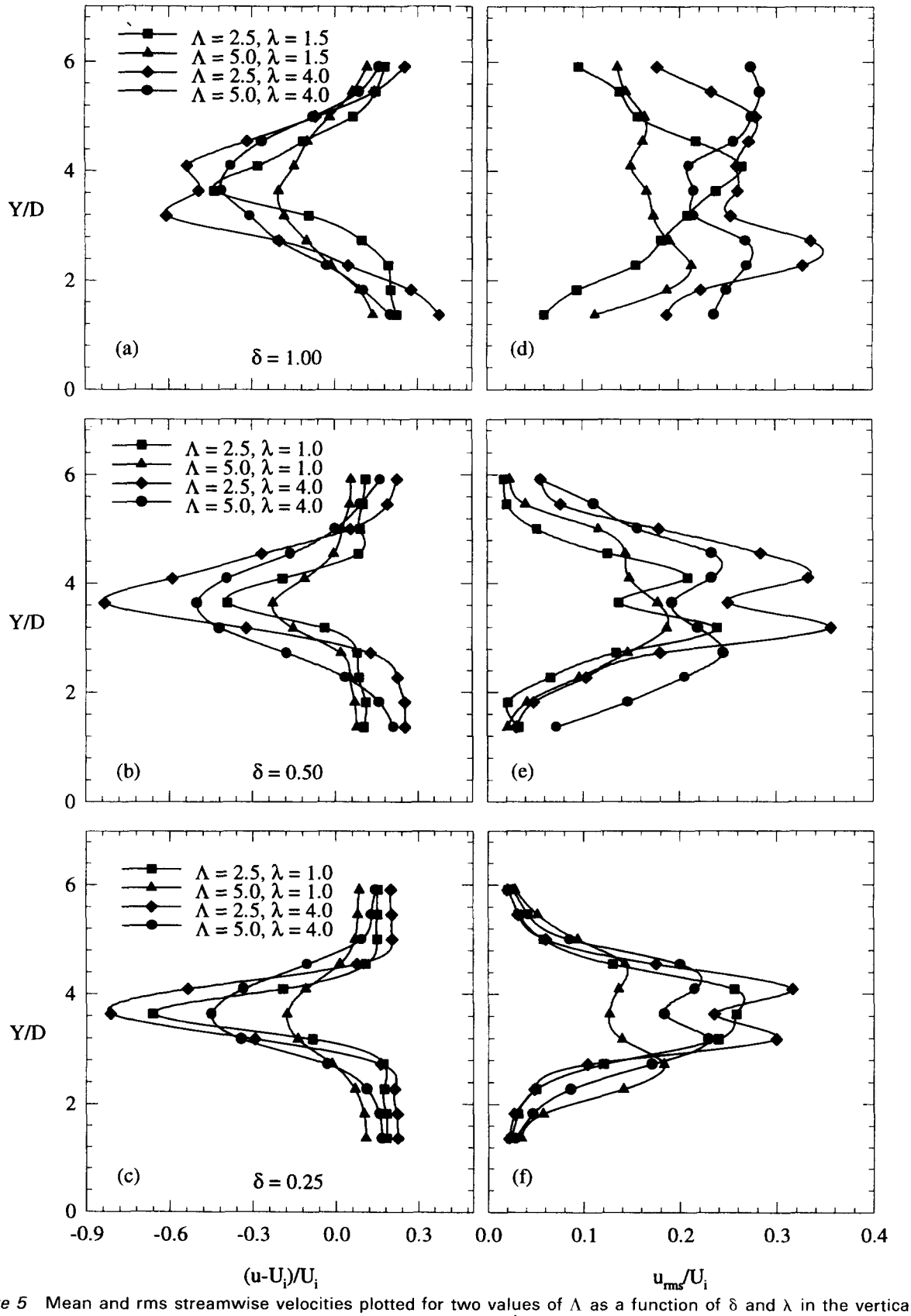

Figure 5 Mean and rms streamwise velocities plotted for two values of Λ as a function of δ and λ in the vertical symmetry plane of the duct for prism pairs with $\alpha = 0.50$ and $Re_D = 1.0 \times 10^4$

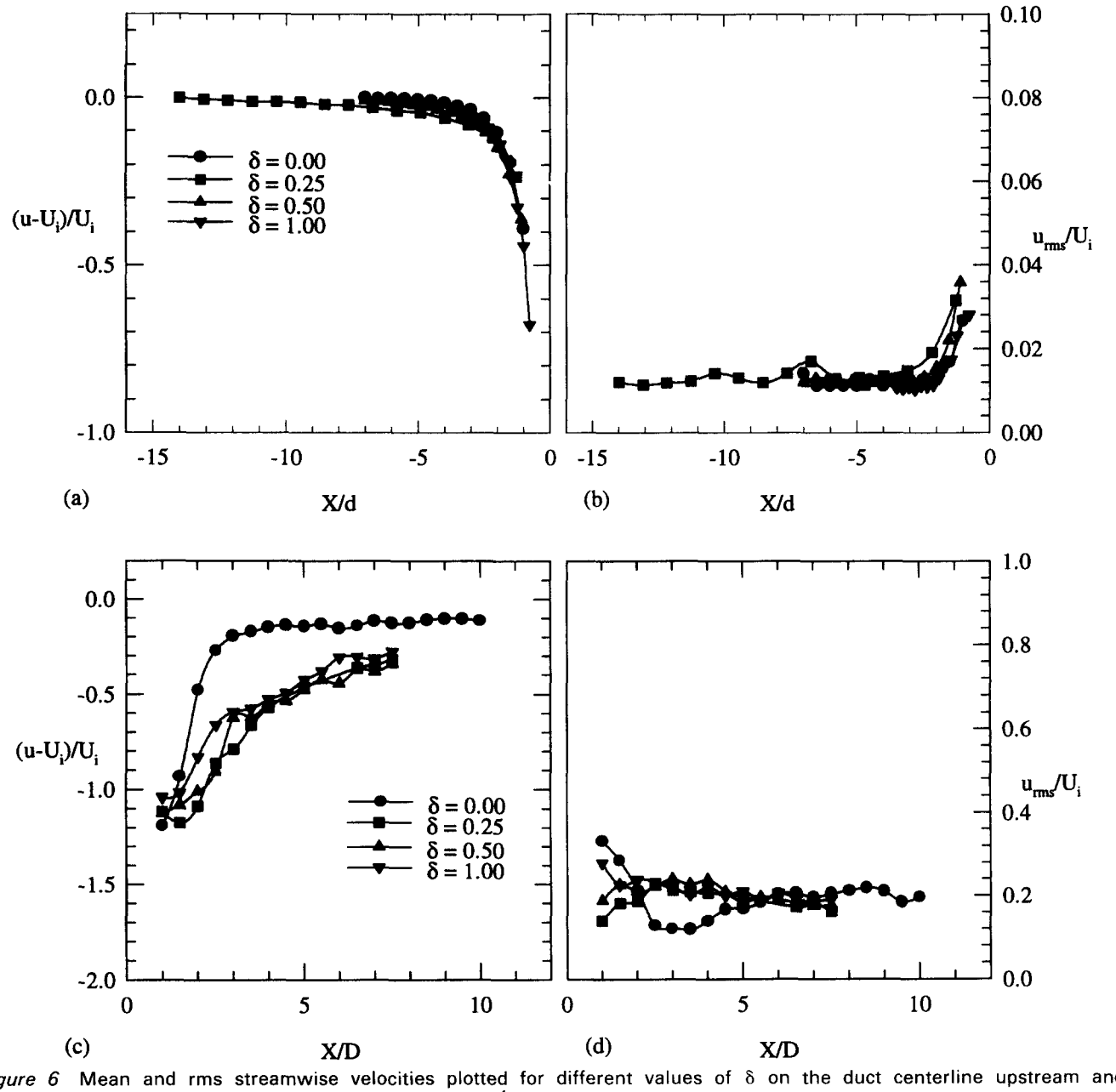

Figure 6 Mean and rms streamwise velocities plotted for different values of δ on the duct centerline upstream and downstream of prism pairs with $\lambda = 4$ and $Re_D = 1.0 \times 10^4$

is negative; that is, directed counter to the bulk flow direction. For larger values of λ, the value of C_D for tandem prisms with $\delta = 1.0$ quickly rises to the single-prism value (2.1 at $Re_D = 1.0 \times 10^4$), while the values for $\delta = 0.25$ and 0.50 level out to $C_D \approx 0.8$. For interprism spacings $\lambda > 2$, decreasing the size of the upstream prism works to significantly reduce the drag on the larger downstream prism, while the converse is true for $\lambda < 2$. In all the tandem-prism cases, the lift coefficient C_L of the downstream prism was zero to within the experimental uncertainty.

The results for the Strouhal number of the downstream prism of a tandem pair show that for $\lambda \approx 1$ this quantity maximizes between $\delta = 0.25$ and 1.00, while for $\delta \approx 1.00$ it minimizes between $\lambda = 1.0$ and 4.0. Although limited, the Strouhal number results support the notions that: (1) the vortex-shedding frequency of the downstream prism of a pair with $\delta \leq 1.0$ differs significantly from that for a single prism due to upstream/downstream prism interactions and (2) the upstream prism of the same pair can drive the vortex-shedding frequency of the downstream prism for certain values of λ. Such observations have also been reported by Zdravkovich (1977) for tandem cylinders.

Acknowledgments

The experiment was performed by the authors at the University of California at Berkeley and the writing of the paper at the University of Arizona. The generous support of the IBM Corporation is gratefully acknowledged. In particular, the keen interest shown by H. Greenberg, R. Linton, and V. Kamath at IBM is deeply appreciated. Thanks go to Sonic Environmental Systems for the donation of the nozzle atomizers used to generate the water mist for the laser-Doppler measurements.

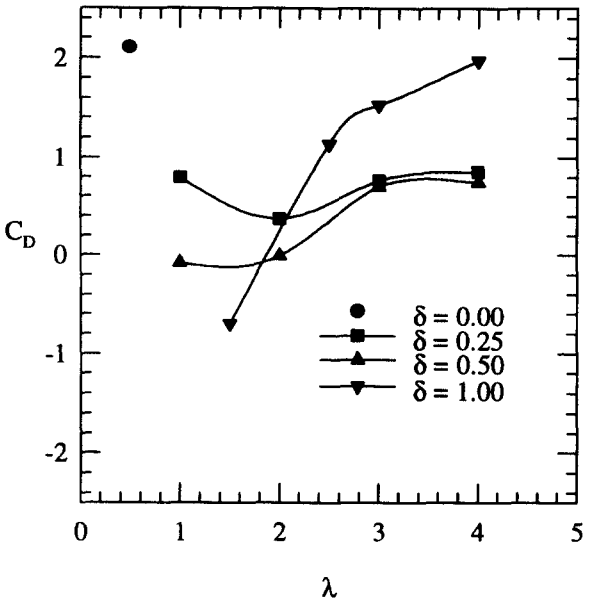

Figure 7 Drag coefficient plotted as a function of λ for different values of δ for the downstream prism (*D*) of a pair with $Re_D = 1.0 \times 10^4$; datum for single prism is shown in the top left corner

References

Albayrak, K. 1991. Design of a low-speed axisymmetric wind tunnel contraction. *J. Wind Eng. Ind. Aerodynamics*, **37**, 79–86

Bearman, P. W., and Obasaju, E. D. 1982. An experimental study of pressure fluctuations on fixed and oscillating square-section cylinders. *J. Fluid Mech.*, **119**, 297–321

Bell, W. A. 1986. Spectral analysis of laser velocimetry data with the slotted correlation method. *Proc. AIAA/ASME 4th Fluid Mechanics, Plasma Dynamics, and Lasers Conference*

Bosch, G. and Rodi, W. 1995. Simulation of vortex shedding past a square cylinder near a wall. *Proc. 10th Symposium on Turbulent Shear Flows*, The Pennsylvania State University, University Park, PA, Vol. 1, 4.13–4.18

Cohen, M. J. and Ritchie, N. B. J. 1962. Low-speed three-dimensional contraction design. *J. Royal Aeronaut. Soc.*, **66**, 231–236

Drain, L. W. 1980. *The Laser Doppler Technique*. Wiley, New York, 136

Devarakonda, R. 1994. Experimental and numerical investigation of unsteady bluff body flows. Ph.D. Thesis, University of California at Berkeley, Berkeley, CA

Durão, D. F. G., Heitor, M. V. and Pereira, J. C. F. 1988. Measurements of turbulent and periodic flows around a square cross-section cylinder. *Exp. Fluids*, **6**, 298–304

Franke, R. and Rodi, W. 1991. Calculation of vortex shedding past a square cylinder with various turbulence models. *Proc. 8th Symposium on Turbulent Shear Flows*, Technical University of Munich, Munich, Germany, Vol. 2, 20.1.1–20.1.6.

Igarashi, T. 1985. Heat transfer from a square prism to an air stream. *Int. J. Heat Mass Transfer*, **28**, 175–181

Igarashi, T. 1986. Local heat transfer from a square prism to an air stream. *Int. J. Heat Mass Transfer*, **29**, 777–784

Igarashi, T. 1987. Fluid flow and heat transfer around rectangular cylinders (The case of a width/height ratio of a section of 0.33–1.5). *Int. J. Heat Mass Transfer*, **30**, 893–901

Kline, S. J. and McClintock, F. A. 1953. Describing uncertainties in single-sample experiments. *Mech. Eng.*, **75**, 3–8

Lee, B. E. 1975. The effect of turbulence on the surface pressure field of a square prism, *J. Fluid Mech.*, **69**, 263–282

Luo, S. C. and Teng, T. C. 1990. Aerodynamic forces on a square section cylinder that is downstream to an identical cylinder. *Aeronaut. J.*, 203–212

Mehta, R. D. and Bradshaw, P. 1979. Design rules for small low-speed wind tunnels. *Aeronaut. J. Royal Aeronaut. Soc.*, 443–449

Moffat, R. J. 1982. Contributions to the theory of single-sample uncertainness analysis. *J. Fluids Eng.*, **104**, 250–260

Okajima, A. 1982. Strouhal numbers of rectangular cylinders. *J. Fluid Mech.*, **123**, 379–398

Ota, T., Nishiyama, H., Kominami, J. and Sato, K. 1986. Heat transfer from two elliptic cylinders in tandem arrangement. *J. Heat Transfer*, **108**, 525–531

Sayers, A. T. 1991. Steady-state pressure and force coefficients for groups of three equispaced square cylinders situated in a cross flow. *J. Wind Eng. Ind. Aerodynamics*, **37**, 197–208

Tatsutani, K., Devarakonda, R., and Humphrey, J. A. C. 1993. Unsteady flow and heat transfer for cylinder pairs in a channel. *Int. J. Heat Mass Transfer*, **36**, 3311–3328

Zdravkovich, M. M. 1977. Review of flow interference between two circular cylinders in various arrangements. *J. Fluids Eng.*, **99**, 618–633

Žukauskas, A. 1972. Heat transfer from tubes in cross flow. *Adv. Heat Transfer*, **8**, 93–160